CHAPTER 144

WAVE FORCES INDUCED BY IRREGULAR WAVES ON A VERTICAL CIRCULAR CYLINDER

Hajime Ishida

Lecturer, Department of Civil Engineering,
Kanazawa University, Kanazawa, Japan

and

Yuichi Iwagaki

Professor, Department of Civil Engineering,
Kyoto University, Kyoto, Japan

ABSTRACT

In order to examine the irregular wave forces on a small diameter cylinder, laboratory experiments have been conducted on water particle velocities and wave forces with various kinds of irregular waves. As the results, it is indicated that the time variation and the spectral distribution of wave forces can be calculated adequately from the water level variations by using the methods proposed by Reid[1] and Borgman[2] respectively.

Moreover, with respect to the irregular wave forces on a large diameter cylinder, a new calculation method was shown by means of applying Reid's linear filters[1] to MacCamy and Fuchs's diffraction theory[3].

INTRODUCTION

A number of studies have been done with respect to wave forces induced by periodic waves on marine structures, especially on a circular cylinder. Considering the irregularity of waves in the fields, however, it is very important to investigate the irregular wave forces systematically. In the case of periodic waves, Morison's equation and MacCamy and Fuchs's diffraction theory have been employed to estimate the wave forces respectively on a small and on a large diameter cylinder. Therefore, in the case of irregular waves, it is reasonable to investigate the wave forces by using these two methods in the same way.

Formerly, Reid has studied of the correlation of water level variations with wave forces on a circular cylinder for nonperiodic waves from the viewpoint of their time variations and indicated a method of calculation for the drag and inertia coefficients in Morison's equation. On the other hand, Borgman has shown a method of calculation for the wave force spectrum from the water level spectrum. These methods, however, have

been supported by experiments not sufficiently. As for the irregular wave forces on a large diameter cylinder, few studies have been presented till now.

Therefore, the authors have studied firstly the water particle velocities[4] in irregular waves, which play an important role in Morison's equation, and secondary the wave forces on a small diameter cylinder from the standpoints of the time variation and the power spectral distribution. Finally we show the method of calculation for irregular wave forces on a large diameter cylinder.

VELOCITIES AND ACCELERATIONS IN IRREGULAR WAVES

1-(1). Experiments

In order to investigate the water particle velocities and accelerations in irregular waves, laboratory experiments were carried out at the Department of Civil Engineering, Kyoto University.

The sketch of this experimental apparatus are shown in Fig.1. The dimension of the wave tank is 50cm wide, 70cm high and 27m long. The generator of irregular waves is installed at the end of the tank. A probe of the ultrasonic current meter shown in Photo.1 and a wave gauge were set 8m apart from the wave plate. At another end of the tank, the wave absorber was installed. The generator of irregular waves has fifteen band-pass filters which divide the frequency range 0.2∿5.0 Hz every 1/3 oct., and therefore, irregular waves having various kinds of spectral distributions can be generated by regulating the output of each filter.

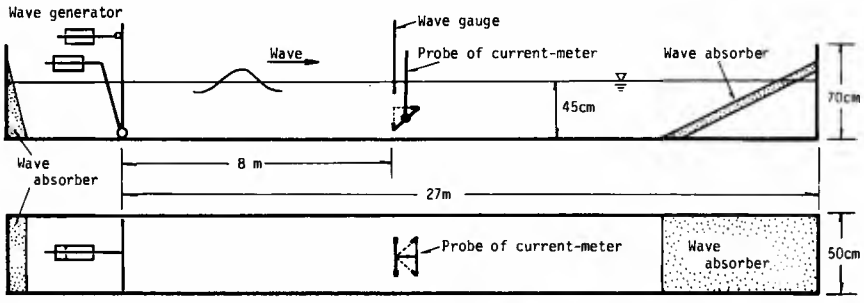

Fig.1 Schematic of experimental apparatus in the case of water particle velocity.

Photo.1 Probe of ultrasonic current meter.

The current meter makes use of the Doppler effect that the velocity of a moving particle is converted into a frequency shift. The relationship between the output voltage and the water particle velocities was determined not only by the electric examination but also by the steady and dynamic calibrations in the tank. Poly vinil chloride powder was used as the material for reflection of ultrasonic waves in water.

In the experiment, the water depth was always kept at 45cm, and the depth of measuring point of water particle velocities were 4.5cm, 9.0cm and 13.5cm below the still water level. Twenty kinds of irregular waves were generated by combining the band pass filters as shown in Table 1. All of the experimental data were recorded by an analog data recorder of magnetic type and digitized by an A-D converter with 0.08 sec time interval.

Table 1 Experimental conditions of water particle velocity.

water depth h=45 cm

Experi. case	Measuring point z (cm)	Frequency and gain of band pass filter (max 10, min 0)														
		.2 (Hz)	.25 (〃)	.315 (〃)	.4 (〃)	.5 (〃)	.63 (〃)	.8 (〃)	1.0 (〃)	1.25 (〃)	1.6 (〃)	2.0 (〃)	2.5 (〃)	3.5 (〃)	4.0 (〃)	5.0 (〃)
I-1	− 9.0					10										
I-2	− 9.0							10								
I-3	− 9.0									10						
I-4	− 9.0										10					
I-5	− 9.0								10	10						
I-6	− 9.0							10	10	10						
I-7	− 9.0							10	10	10	10					
I-8	− 9.0					10	10	10	10							
I-9	− 9.0					10	10	10	10	10	10					
I-10	− 9.0					10	10	10	10	10	10	10				
I-11	− 9.0					4	7	9	10	10	9	7	4			
I-12	− 9.0	10	10	10	10	10	10	10	10	10	10	10	10			
I-13	− 9.0	10	10	10	10							10	10			
I-14	− 9.0						10	10	10	10	10					
I-15	− 4.5					4	7	9	10	10	9	7	4			
I-16	− 4.5	10	10	10	10	10	10	10	10	10	10	10	10			
I-17	− 4.5	10	10	10	10	10	10	10	10	10	10	10	10	10	10	10
I-18	−13.5					4	7	9	10	10	9	7	4			
I-19	−13.5	10	10	10	10	10	10	10	10	10	10	10	10			
I-20	−13.5	10	10	10	10	10	10	10	10	10	10	10	10	10	10	10

1-(2). Analysis

Let the position of a wave gauge across the still water surface be taken as the origin of the coordinates, the direction of wave propagation as X-axis, and the vertical direction upward as Z-axis, respectively. If the water surface elevation of irregular waves at the position of a wave gauge is represented as

$$\eta(t)=\int_0^\infty M(\omega)\cos(\omega t-\theta(\omega))d\omega \quad , \quad \cdots\cdots\cdots\cdots\cdots\cdots (1)$$

the horizontal velocity u and vertical velocity w of a water particle, and the horizontal and vertical acceleration, $\dot{u}$ and $\dot{w}$, are represented as follows[1] by using the small amplitude wave theory:

$$u(t)=\int_0^\infty R_u(\omega)M(\omega)\cos(\omega t-\theta(\omega))d\omega \quad , \quad \cdots\cdots\cdots\cdots\cdots\cdots (2)$$

$$w(t)=-\int_0^\infty R_w(\omega)M(\omega)\sin(\omega t-\theta(\omega))d\omega \quad , \quad \cdots\cdots\cdots\cdots\cdots\cdots (3)$$

$$\dot{u}(t)=-\int_0^\infty \omega R_u(\omega)M(\omega)\sin(\omega t-\theta(\omega))d\omega \quad , \quad \cdots\cdots\cdots\cdots\cdots\cdots (4)$$

$$\dot{w}(t)=-\int_0^\infty \omega R_w(\omega)M(\omega)\cos(\omega t-\theta(\omega))d\omega \quad , \quad \cdots\cdots\cdots\cdots\cdots\cdots (5)$$

in which ω is the angular frequency, θ is the initial phase, $M(\omega)$ corresponds to the amplitude spectrum, and $R_u(\omega)$ and $R_w(\omega)$ are given by

$$R_u(\omega)=\frac{\omega\cosh k(h+z)}{\sinh kh} \quad , \quad \cdots\cdots\cdots\cdots\cdots\cdots (6)$$

$$R_w(\omega)=\frac{\omega\sinh k(h+z)}{\sinh kh} \quad , \quad \cdots\cdots\cdots\cdots\cdots\cdots (7)$$

$$\omega^2=gk\tanh kh \quad , \quad \cdots\cdots\cdots\cdots\cdots\cdots (8)$$

in which h is the water depth and k is the wave number.

Eqs.(6) and (7) give the theoretical frequency responce functions of u and w to η, while experimental values of them are calculated from

$$R_u=\sqrt{\frac{S_u(\omega)}{S_\eta(\omega)}} \quad , \quad \cdots\cdots\cdots\cdots\cdots\cdots (9)$$

$$R_w=\sqrt{\frac{S_w(\omega)}{S_\eta(\omega)}} \quad , \quad \cdots\cdots\cdots\cdots\cdots\cdots (10)$$

in which $S_\eta(\omega)$, $S_u(\omega)$ and $S_w(\omega)$ are the power spectra of η, u and w respectively.

In order to calculate the time variations of u and $\dot{u}$ from η, Reid proposed the following symmetrical and asymmetrical linear filters[1]:

$$G_s[y(t)]=a_0y(t)+\sum_{n=1}^{N}a_n[y(t+n\tau)+y(t-n\tau)] \quad , \quad \cdots\cdots\cdots\cdots (11)$$

$$G_a[y(t)]=\sum_{n=1}^{N}b_n[y(t+n\pi)-y(t-n\tau)] \quad , \quad \cdots\cdots\cdots\cdots\cdots (12)$$

in which a_n and b_n are Fourier coefficients of their frequency responce functions. Substituting $\eta(t)$ of Eq.(1) into $y(t)$ in Eqs.(11) and (12), they are deduced as follows:

$$G_s[\eta(t)]=\int_0^\infty [a_0+2\sum_{n=1}^{N} a_n \cos n\omega\tau]M(\omega)\cos(\omega t-\theta(\omega))d\omega \quad , \quad \cdots\cdots\cdots(13)$$

$$G_a[\eta(t)]=-\int_0^\infty [2\sum_{n=1}^{N} b_n \sin n\omega\tau]M(\omega)\sin(\omega t-\theta(\omega))d\omega \quad . \quad \cdots\cdots\cdots(14)$$

Comparing Eq.(1) with Eqs.(13) and (14), it is found that G_S produces no phase change and has the frequency responce function $[a_0+2\sum_{n=1}^{N} a_n \cos n\omega\tau]$, and that G_a changes the phase by $\pi/2$ and has $[2\sum_{n=1}^{N} b_n \sin n\omega\tau]$ as the frequency responce function. It is also seen by comparing Eqs.(2) to (5) with Eqs. (13) and (14) that the time variations of required variables can be calculated from the water level variation $\eta(t)$ by selecting one of the frequency responce functions and filters as shown in Table 2. In the calculation, τ=0.08 sec and N=25 were adopted.

As the acceleration can not be measured directly, $\dot{u}$ and $\dot{w}$ are estimated by differentiating measured u and w with respect to time t. However, since the direct differentiation may enlarge errors due to noises more or less contained in measured u and w, they are differentiated after being passed through the following low-pass filter:

$$F_c(\omega)=\begin{cases} 1: \omega\leqq 2\pi f_c \\ 0: \omega>2\pi f_c \end{cases} \quad . \quad \cdots\cdots\cdots\cdots\cdots(15)$$

In actual calculations, this operation was carried out by using the filter G_S which has the frequency responce function $\omega F_C(\omega)$. In the calculation, f_C=4.0 Hz, τ=0.08 sec and N=40 were used.

Table 2 Correspondence of input, frequency response function and linear filter to output.

Input	Frequency response function	Linear filter	Output
Measured $\eta(t)$	$R_u(\omega)$	$G_s[\eta(t)]$	$u(t)$
	$\hat{R}_w(\omega)$	$G_a[\eta(t)]$	$w(t)$
	$\omega R_u(\omega)$	$G_a[\eta(t)]$	$\dot{u}(t)$
	$-\omega R_w(\omega)$	$G_s[\eta(t)]$	$\dot{w}(t)$
Measured $u(t)$	$\omega F_c(\omega)$	$G_a[u(t)]$	$\dot{u}(t)$
Measured $w(t)$		$G_a[w(t)]$	$\dot{w}(t)$

1-(3). Results and discussions

As an example, the results of Case I-10 are shown in Figs.2 through 9. In Fig.2, the power spectral densities S_η, S_u and S_w of η, u and w respectively are compared. In the frequency range for the large value of S_η, three power spectra resemble each other in shape. However, in the high frequency range (>1.5 Hz), the values of S_w become larger than those of S_u. This trend is seen in all cases. In the range of higher frequency than 2 Hz, the accuracy of the current meter becomes poor, so that the noise of the current meter can not be separated from the power of u and w.

Therefore, more detailed discussion on the characteristics of the high frequency components of u and w has no meaning.

In Figs.3 and 4, experimental values of the frequency responce functions calculated from Eqs.(9) and (10) are compared with the theoretical values by Eqs.(6) and (7) based on the small amplitude wave theory. In the low frequency range (<1.5 Hz), the experimental values agree well with the theoretical curves, but in the high frequency range (>1.5 Hz), the former becomes larger than the latter.

Fig.5 shows an example of the time variation of measured η of irregular waves. Calculated values of u, w, $\dot{u}$ and $\dot{w}$ obtained by using measured η as an input to each linear filter (in Table 2) are plotted in Figs.6 through 9. Fig.6 shows the comparison between time variations of the measured u and the simultaneously calculated one. Both are in good agreement, but the measured value is slightly larger than the calculated one near the crest and trough. In Fig.7, the time variation of measured w is compared with that of the simultaneously calculated one. In the vicinity of the trough the measured value is larger than the calculated one. Also the level of noise of the current meter in w is higher than that in u.

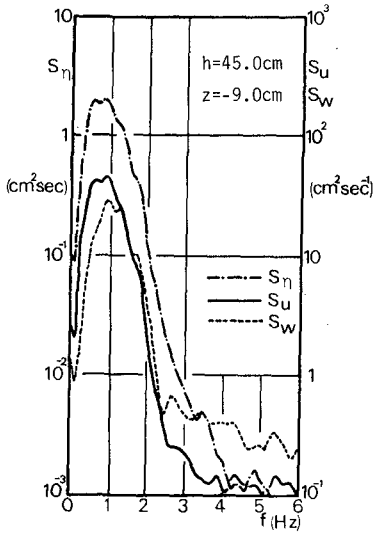

Fig.2 Power spectral density distribution of η, u and w of irregular waves.

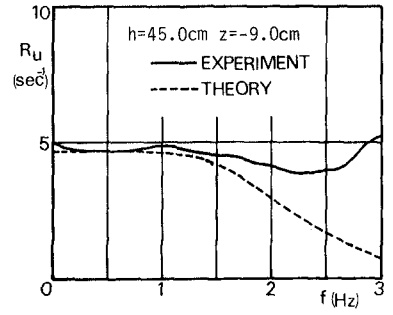

Fig.3 Frequency responce function of u to η under irregular waves.

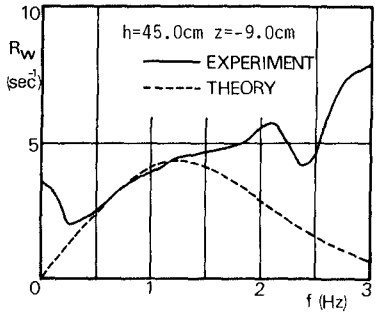

Fig.4 Frequency responce function of w to η under irregular waves.

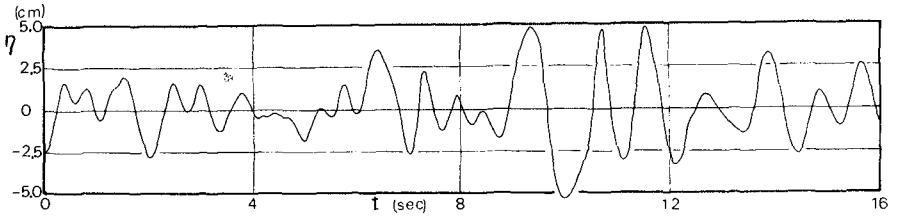

Fig.5 Time variation of η of irregular wave.

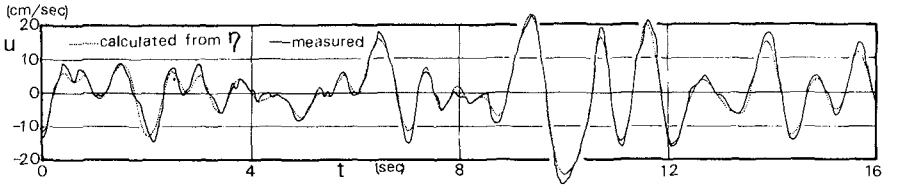

Fig.6 Time variation of u in irregular wave.

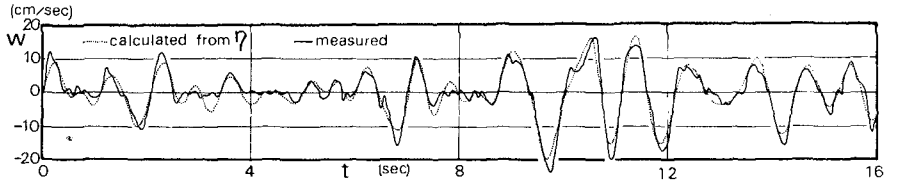

Fig.7 Time variation of w in irregular wave.

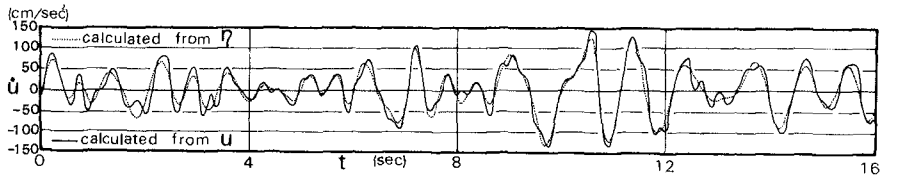

Fig.8 Time variation of $\dot{u}$ in irregular wave.

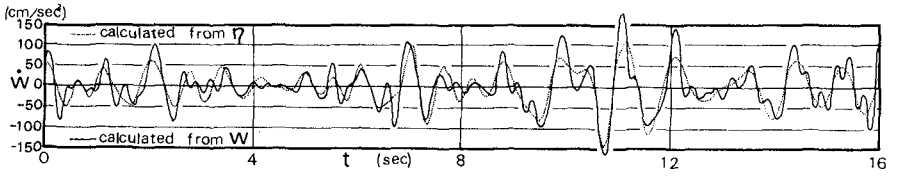

Fig.9 Time variation of $\dot{w}$ in irregular wave.

Fig.8 shows the comparison of the time variation of $\dot{u}$ between that calculated from the time variation of η and that calculated from the measured u by passing it through the filter which has the frequency responce function $\omega F_c(\omega)$ shown in Table 2. Both are in fairly good agreement, and however, since the measured u contains some noises, high frequency disturbances are seen in the curve of $\dot{u}$ calculated from the measured u, even though it is passed through the low-pass filter $F_c(\omega)$. Fig.9 also shows the comparison of the time variation of $\dot{w}$ between calculated from the measured η and calculated from the measured w. Higher level noises are contained in this case than in the case of u, so that the high frequency vibration in $\dot{w}$ calculated from w is larger than that in $\dot{u}$ calculated from u.

The discussion mentioned above is only for Case I-10. Now considering all cases of the irregular waves shown in Table 1, the following facts are obtained:

Regardless of the shape of power spectrum of water level variation, the measured value of frequency responce function for the water particle velocity agrees well with the theoretical value based on the small amplitude wave theory in the low frequency range where the value of S_η is large. On the other hand, in the high frequency range, the measured value of the frequency responce function becomes larger than the theoretical value. This trend is remarkable for w. This may explain the experimental fact that absolute values of measured time variations of u and w near the wave crest and trough, where the effect of high frequency components will appear, become larger than those calculated by the linear filters.

In the water particle accelerations, $\dot{u}$ and $\dot{w}$, calculated from the measured u and w, there are bigger high frequency disturbances than in the case of $\dot{u}$ and $\dot{w}$ obtained from η. This is due to noises originally contained in measured u and w. However, relatively low noise level in u makes the difference between $\dot{u}$ calculated by the two methods small, while the difference is big in the case of $\dot{w}$ because of higher noise level.

The cut-off frequency of the low-pass filter, f_c, was 4.0 Hz in the calculation of Eq.(15). If we select a smaller f_c, noises are expected to be reduced. However, since the cause of the noise is a defect of the current meter itself, only the improvement of the current meter in future can solve this problem.

IRREGULAR WAVE FORCES ON A SMALL DIAMETER CYLINDER

2-(1). Experiments

In order to estimate irregular wave forces on a small diameter cylinder by using Morison's equation, laboratory experiments were carried out for 22 kinds of irregular waves in the same wave tank as mentioned in 1-(1).

The disposition of the experimental apparatus are also shown in Fig. 10. A wave gauge, the current meter and a circular cylinder were set 6m apart from the wave plate. The cylinder is 6cm in diameter and constracted of three parts, the upper and the lower cylinder and the segment with length of 4cm, as shown in Fig.11.

The data on wave forces on the segment are obtained by using the two strain gauges attached to the plate spring which suspends the segment from the upper cylinder. The natural frequency of this system in the still

water was 19.2 Hz. This frequency was so high as to avoid the experimental error caused by interactions of the segment to the waves.

In the experiment, the water depth was 45cm, and the depth of measuring point of wave forces were 10cm, 15cm and 20cm below the still water level. All of experimental data were recorded by the analog data recorder with 0.08 sec and 0.02 sec time interval.

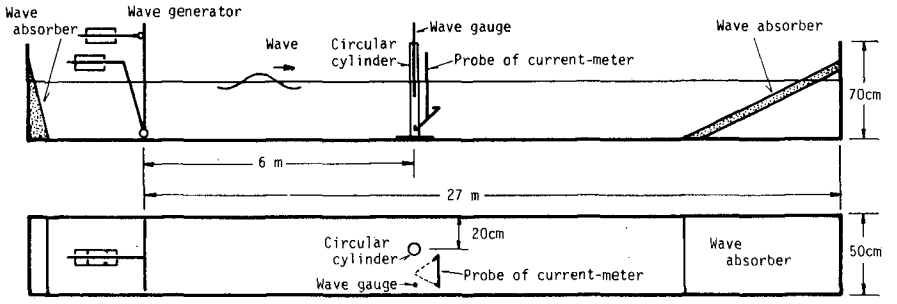

Fig.10 Schematic of experimental apparatus in the case of wave force.

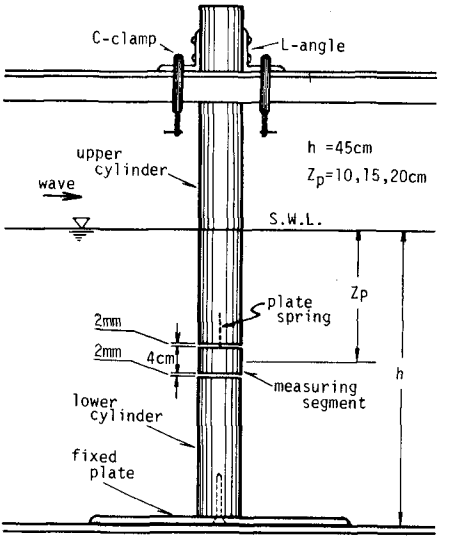

Fig.11 Schematic of circular cylinder.

2-(2). Analysis

The method of calculation for the time variation of irregular wave forces has been also shown by Reid as described below[1]:

Irregular wave forces as well as periodic ones can be expressed by the following Morison's equation:

$$F(t)=C_D\cdot\frac{\rho}{2}Du(t)|u(t)|+C_M\cdot\rho\frac{\pi D^2}{4}\dot{u}(t) \quad , \quad \cdots\cdots\cdots(16)$$

in which ρ is the density, D is the diameter of cylinder, C_D and C_M are the drag and inertia coefficients respectively, and $u(t)$ and $\dot{u}(t)$ can be calculated from the following Eqs.(17) and (18):

$$C_D=\overline{F^*(t)\cdot F_1(t)}/\overline{F_1(t)^2}, \quad \cdots\cdots\cdots\cdots(17)$$

$$C_M=\overline{F^*(t)\cdot F_2(t)}/\overline{F_2(t)^2} \quad . \quad \cdots\cdots\cdots\cdots(18)$$

These eqations have been obtained by using the condition that the value of the variance between the measured wave force $F^*(t)$ and $F(t)$ of Eq.(16) is made least, in which $F_1(t)$ and $F_2(t)$ are respectively the drag and the inertia wave force in Eq.(16), and $\overline{\quad}$ indicates to take the avarage with respect to time t. The degree of differences between $F^*(t)$ and $F(t)$ can be known from their correlation coefficient r shown by the following equation:

$$r=\sqrt{1-[\overline{\{F(t)-F^*(t)\}^2}/\overline{F^*(t)^2}]} \quad . \quad \cdots\cdots\cdots(19)$$

This Reid's method was applied to all of experimental cases to obtain the values of C_D and C_M, and moreover, these values were employed to Eq.(16) to compare with $F^*(t)$ from the viewpoint of time variation. In the calculation, τ=0.02 sec and N=40 were used.

On the other hand, the spectral distribution of wave forces, $S_F(f)$, can be calculated from the spectrum of water level variation, $S_\eta(f)$, by using the following equations obtained by Borgman[2]:

$$S_{F1}(f)=\frac{8d^2\sigma^2}{\pi}S_u(f)+m'^2S_{\dot{u}}(f) \quad , \quad \cdots\cdots\cdots\cdots(20)$$

$$S_{F2}(f)=\frac{d^2\sigma^2}{\pi}\left[\frac{8}{\sigma^2}S_u(f)+\frac{4}{3\sigma^6}[S_u(f)]^{*3}\right]+m'^2S_{\dot{u}}(f) \quad , \quad \cdots\cdots(21)$$

$$\left.\begin{aligned} &d=C_D\cdot\frac{1}{2}\rho D \ , \ m'=C_M\cdot\frac{1}{4}\rho\pi D^2, \ \sigma^2=2\int_0^\infty S_u(f)\,df \ , \\ &[S_u(f)]^{*3}=\int_{-\infty}^{\infty}[S_u(g)]^{*2}S_u(f-g)\,dg \ , \\ &[S_u(f)]^{*2}=\int_{-\infty}^{\infty}S_u(g)S_u(f-g)\,dg \ , \end{aligned}\right\}\cdots\cdots(22)$$

in which f is the frequency, and $S_{F_1}(f)$ and $S_{F_2}(f)$ are respectively the first and the second approximation of wave force spectrum.

These equations were also applied to all of experimental cases and compared with the spectra, $S_{F^*}(f)$, obtained from the measured wave force F^*. In the calculation of S_{F_1} and S_{F_2}, it is necessary to give the values of C_D and C_M, and therefore, the values obtained from Eqs.(17) and (18) were employed. As for the calculation of S_η and S_{F^*}, the data with time interval 0.08 sec were used.

2-(3). Results and discussions

Table 3 shows the experimental cases of irregular wave forces, in which z_p is the depth of the measuring point, (Wave freq.(Hz)) is the frequency range of band pass-filters employed to generate the waves, and C_D, C_M and r are respectively the drag, the inertia and the correlation coefficients calculated from Eqs.(17), (18) and (19) respectively. The values of C_D and C_M are respectively from 5.60 to 1.45 and from 2.30 to 1.51, and seem to become larger in both cases that z_p is closer to the water surface and that the generated waves shown by (Wave freq.(Hz)) contain higher frequency component waves more powerfully. In irregular waves, as the measuring point become closer to the water surface, high frequency components of water particle velocities increase even if the frequency components of surface waves are not changed. Therefore, this trend may be generalized by the statement that the values of C_D and C_M increase according to increase in high frequency components of water particle velocities.

Table 3 Values of C_D, C_M and r in each experimental Case.

$h = 45$ cm

Case	z_p (cm)	Wave freq. (Hz)	C_D	C_M	r
1		(0.5)	1.74	1.98	0.948
2		(0.8)	2.74	2.15	0.965
3		(1.0)	3.94	2.15	0.971
4		(1.25)	4.85	2.27	0.977
5	−10	(0.2~1.0)	2.33	2.03	0.960
6		(0.8~1.25)	4.10	2.13	0.956
7		(0.5~1.6)	4.21	2.30	0.947
8		(0.4~2.5)	5.60	2.29	0.955
9		(0.2~5.0)	2.66	2.08	0.945
10		(0.8)	2.70	1.92	0.971
11		(1.0)	2.74	1.94	0.980
12		(0.2~1.0)	2.19	1.95	0.966
13	−15	(0.8~1.25)	2.60	2.04	0.975
14		(0.5~1.6)	2.56	2.02	0.961
15		(0.4~2.5)	2.26	1.88	0.962
16		(0.2~5.0)	2.62	1.99	0.967
17		(0.8)	1.46	1.57	0.958
18		(0.2~1.0)	1.85	1.53	0.959
19		(0.8~1.25)	2.06	1.64	0.966
20	−20	(0.5~1.6)	2.38	1.63	0.962
21		(0.4~2.5)	1.71	1.51	0.958
22		(0.2~5.0)	1.45	1.57	0.956

The reasons why such tendencies appear are not necessarily clear now, but some discussions can be made as follows[5]:

When the water particle velocities increase in high frequency components, each wave in one series of irregular waves tends to decrease the value of Keulegan-Carpenter's number[6] because smaller period of each wave is more possible. In such a case, the values of C_M become relatively larger because the reduction of the inertia force by wake vortices become smaller. Under such fluid conditions, the drag force may not become so large as to matter in practical application even if the values of C_D become large.

On the other hand, when the increase in high frequency components of velocities is caused by the increase in any nonlinearity not to be expressed by the superposition of small amplitude waves, the velocities and accelerations calculated from η by Reid's method may become a little smaller than actual ones, which may involve some risk of providing larger values of C_D and C_M. Therefore, the characteristics of C_D and C_M in irregular waves are still to be investigated.

As examples of the time variation of irregular wave forces, the results of Cases 5, 14 and 19 (in Table 3) are respectively shown in Fig.12 (a), (b) and (c). The calculated wave forces F shown in chain lines agree fairly well with the measured values F* shown in solid lines, which is also recognized from the fact that almost values of r in Table 3 are close to 1. Strictly speaking, however, F* is slightly larger than F near the crest and trough as well as the velocity and acceleration. The difference of F from F* is caused by not only the differences of calculated u and $\dot{u}$ from their measured ones but also the method of calculation such that C_D and C_M are fixed to certain values over one series of irregular waves.

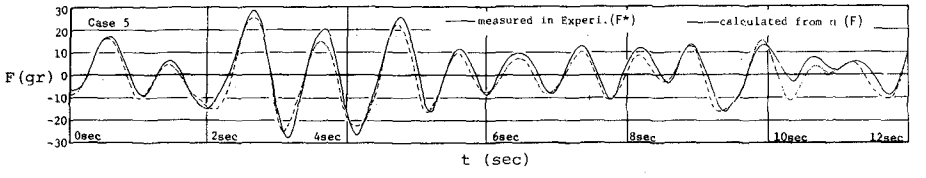

(a) Case 5

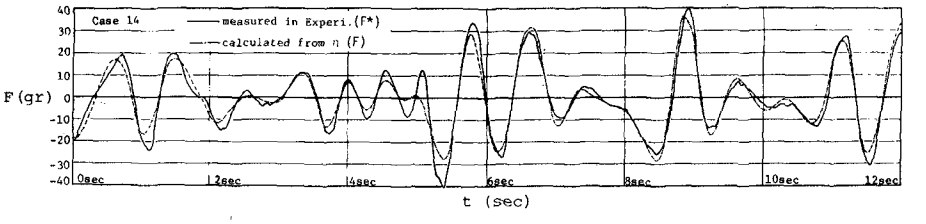

(b) Case 14

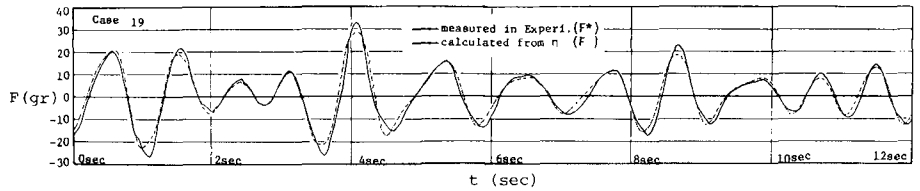

(c) Csae 19

Fig.12 Time variation of wave forces, F* and F, on small cylinder.

As examples of power spectral density distributions of wave forces, the results of Cases 3, 7, 14 and 19 (in Table 3) are shown in Fig.13(a), (b), (c) and (d) respectively. In each figure, the spectrum of the measured wave force, S_{F*}, are shown in solid line, and the first and second approximations of theoretical spectrum, S_{F_1} and S_{F_2}, calculated from S_η by using Eqs.(20) and (21) respectively are shown in dotted lines.

S_{F_2} contains the effect of nonlinear interactions of component waves with each other, but S_{F_1} and S_{F_2} are not so different from each other, and agree well with S_{F*}.

Then, considering the results of all experimental cases shown in Table 3, the following facts are obtained:

The time variations of wave forces calculated from Reid's method are in fairly good agreement with the measured wave forces, and the spectral distributions of forces calculated from Borgman's method also agree well with ones obtained from the measured wave forces.

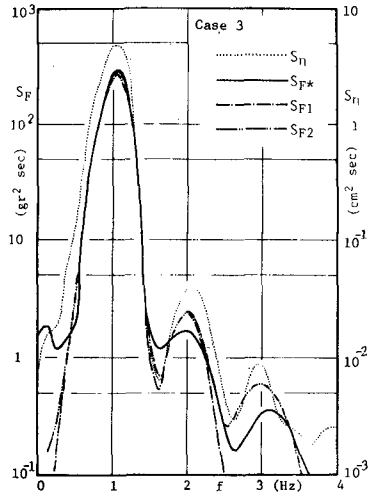

(a) Case 3

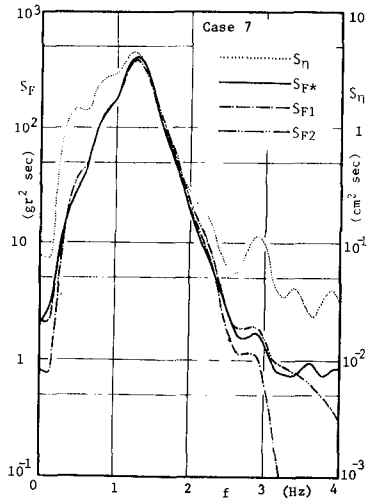

(b) Case 7

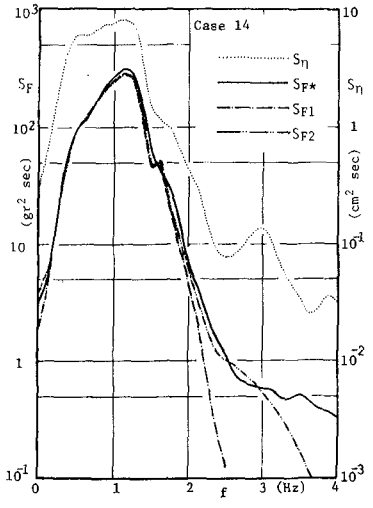

(c) Case 14

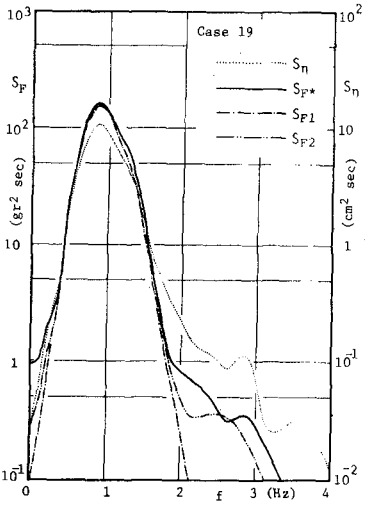

(d) Case 19

Fig.13 Power spectral density distributions, S_{F*}, S_{F_1}, S_{F_2} and S_η.

IRREGULAR WAVE FORCES ON A LARGE DIAMETER CYLINDER

3-(1). Theory

The coordinate system is taken in the same way as mentioned in 1-(2), and moreover, the center axis of a cylinder is at X=0.

When the water level variation at X=0 is monocromatic as shown in Eq.(23), the induced wave force is represented as shown in Eq.(24) by MacCamy and Fuchs's diffraction theory[3]:

$$\eta(t) = a\cos(\omega t - \delta) \quad , \quad \cdots\cdots\cdots\cdots\cdots\cdots (23)$$

$$F(t) = \mathrm{Re}\left\{4\rho g \frac{\cosh k(h+z)}{k\cosh kh} \frac{1}{H_1^{(1)'}(kR)} a e^{-i(\omega t-\delta)}\right\}$$

$$= 4\rho g \cdot C_1(\omega)\cdot a\cos(\omega t - \delta)$$

$$- 4\rho g \cdot C_2(\omega)\cdot a \sin(\omega t - \delta) \quad , \quad \cdots\cdots\cdots\cdots\cdots\cdots (24)$$

in which a is the amplitude, δ is the initial phase, g is the acceleration of gravity, $H_1^{(1)\prime}$ is the derivative of Hankel function of first kind of order 1, and C_1 and C_2 can be deduced as Eqs.(25) and (26) respectively, which become frequency responce functions of wave forces to water level variations:

$$C_1(\omega)=\frac{\cosh k(h+z)}{k\cosh kh}\quad\frac{J_1'(kR)}{J_1'^2(kR)+Y_1'^2(kR)}\quad,\quad\cdots\cdots\cdots\cdots(25)$$

$$C_2(\omega)=\frac{\cosh k(h+z)}{k\cosh kh}\quad\frac{Y_1'(kR)}{J_1'^2(kR)+Y_1'^2(kR)}\quad,\quad\cdots\cdots\cdots\cdots(26)$$

in which R is the radius of the cylinder and J_1' and Y_1' denote the derivatives respectively of Bessel function of order 1 and of Neuman function of order 1.

In the next place, when the water level variation is irregular as shown in Eq.(27), the induced wave force is represented as Eq.(28) within the range of small amplitude wave theory:

$$\eta(t)=\int_0^\infty M(\omega)\cos(\omega t-\delta(\omega))\,d\omega\quad,\quad\cdots\cdots\cdots\cdots\cdots(27)$$

$$F(t)=4\rho g\int_0^\infty C_1(\omega)\cdot M(\omega)\cos(\omega t-\delta(\omega))\,d\omega$$

$$-4\rho g\int_0^\infty C_2(\omega)\cdot M(\omega)\sin(\omega t-\delta(\omega))\,d\omega\quad.\quad\cdots\cdots\cdots(28)$$

The first term in the right hand side of Eq.(28) has the same phase as Eq.(27) and the second term has the changed phase by $\pi/2$ from Eq.(27). Therefore, the time variation of wave forces can be calculated from the simultaneous water level variation by using both the symmetrical linear filter G_s which has the frequency responce function $C_1(\omega)$ and the asymmetrical one G_a which has $C_2(\omega)$, as follows:

$$F(t)=4\rho g G_s[\eta(t)]+4\rho g G_a[\eta(t)]\quad.\quad\cdots\cdots\cdots(29)$$

The validity of this calculation method were discussed by using the wave force data obtained in the experiment with the small diameter cylinder shown in 2-(1).

3-(2). Results and discussions

Figs.14 and 15 show the results obtained by applying the method shown in 3-(1) to Cases 3 and 7 shown in Table 3 respectively, in which, (a) shows the water level variation η used as the input data, and (b) shows the comparison between the measured wave force F^* and the calculated one F obtained as the output data. It is recognized from Fig.14(b) that the calculated wave force shown in chain line agrees well with the

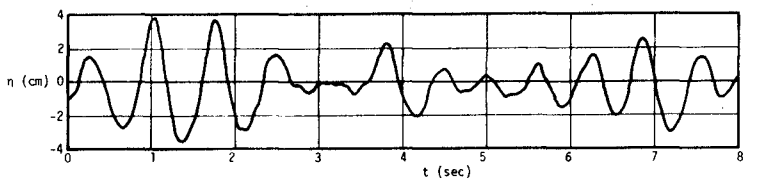

(a) Water level variation

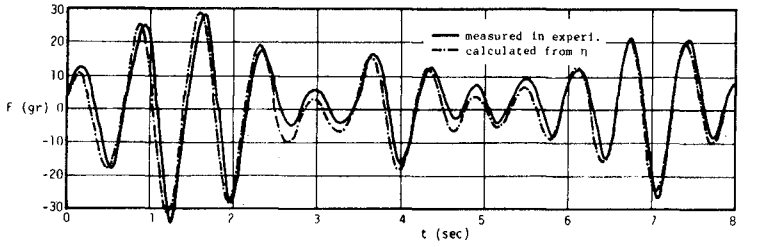

(b) Wave Force

Fig.14 Time variation of wave forces on large cylinder (Case 3)

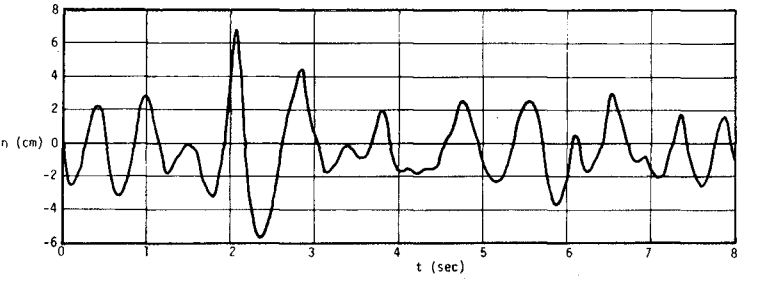

(a) Water level variation

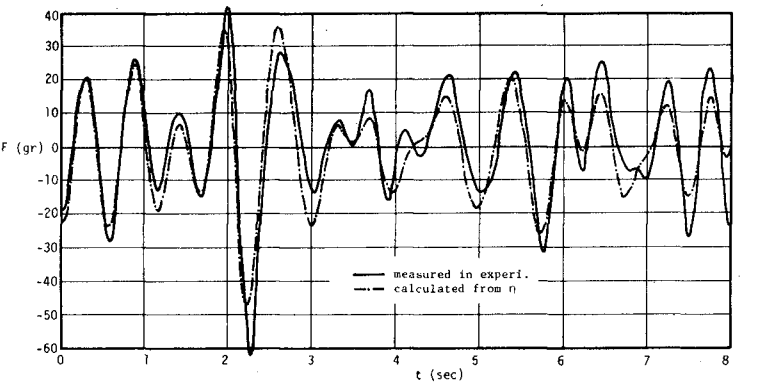

(b) Wave force

Fig.15 Time variation of wave forces on large cylinder (Case 7)

experimental one shown in solid line. This reason is considered that since the waves of Case 3 have the narrow band spectrum of which predominant frequency is relatively high value 1.0 Hz as shown in Fig.13(a), the drag force can be ignored. In another words, the difference between these two curves shows the drag force because the wave force calculated from the diffraction theory expresses only the inertia force.

On the other hand, Fig.15(b) indicates that the calculated wave force is fairl different from the experimental one because of the larger drag force. The reason of the increase in drag force may be understood from its wave spectra shown in Fig.13(b).

Now, considering the results of not only Cases 3 and 7 but also another cases, the following fact is obtained:

When the cylinder is so large in diameter that the inertia wave force is predominant to the drag one, the irregular wave forces can be estimated from only the water level variation by using this method.

CONCLUSION

The time variation of the horizontal and vertical velocities and accelerations of water particles can be predicted fairly well from the water level variation by using Reid's linear filters based on the small amplitude wave theory. Consequently, the time variation of the irregular wave forces can be adequately calculated from the water level variation by using Morison's equation in the case when the values of drag and inertia coefficients can be estimated. In such a case, also the spectral density distribution of wave forces can be calculated adequately from the spectrum of water level variation by using Borgman's method. In order to put these methods into practical application, however, the characteristics of the values of drag and inertia coefficients should be investigated from the standpoint, for example, of comparing with the results already obtained under periodic waves.

On the other hand, in such a case that each wave steepness in irregular waves becomes so large that the nonlinear characteristics can not be ignored, the linear filters may provide a little smaller values of the velocities and accelerations than the actual ones, which involve some risk of providing larger values of drag and inertia coefficients. Therefore, a certain nonlinear filters should be investigated in futuer.

Moreover, when the inertia wave force is predominant to the drag one, irregular wave forces on a cylinder can be calculated from only the water level variation by the method of applying Reid's linear filters to MacCamy and Fuchs's diffraction theory as presented in this paper.

ACKNOWLEDGEMENT

The authors wish to express their gratitude to Mr. Tetsuo Sakai, Mr. Tetsuo Senda and Mr. Yoshiteru Dobashi for their assistance through the experiments and data analysis. This work was partly supported by Scientific Research Funds from the Ministry of Education, Japan.

REFERENCES

1) Reid,R.O., "Correlation of water level variations with wave forces on a vertical pile for nonperiodic waves", Proc. 6th Conf. Coastal Eng., pp.749-786, 1957.

2) Borgman,L.E., "The spectral density for ocean wave forces", Proc. Special Conf. Coastal Eng., pp.147-182, 1965.

3) MacCamy,R.C. and Fuchs,R.A., "Wave forces on piles: Diffraction theory", Tech. Memo, No.69, B.E.B., pp.1-17, 1954.

4) Iwagaki,Y., Sakai,T. and Ishida,H., "Correlation of water particle velocity with water level variation for irregular waves", Coastal Eng. in Japan, Vol.16, pp.19-28, 1973.

5) Iwagaki,Y. and Ishida,H., "Flow separation, wake vortices and pressure distribution around a circular cylinder under oscillatory waves", Proc. 15th Conf. on Coastal Eng., pp.2341-2356, 1976.

6) Keulegan,G.H. and Carpenter,L.H., "Forces on cylinders and plates in an oscillating fluid", Jour. Res. Nat. Bur. Stand., Vol.60, No.5, pp.423-440, 1958.